

**RERTR 2014 – 35TH INTERNATIONAL MEETING ON
REDUCED ENRICHMENT FOR RESEARCH AND TEST REACTORS**

**OCTOBER 12-16, 2014
IAEA VIENNA INTERNATIONAL CENTER
VIENNA, AUSTRIA**

**Validation of the Fuel Plate Swelling Models used in the
Multi-Physics Simulation of the E-FUTURE-1 Fuel Irradiation
Experiment**

A.M. Tentner, A. Bergeron, Y.S. Kim, G.L. Hofman, J.G. Stevens
Nuclear Engineering Division
Argonne National Laboratory, 9700 S. Cass Ave., Argonne IL 60439 – USA

and

S. Van den Berghe¹, V. Kuzminov²

1 - Institute for Nuclear Materials Science, Microstructural and Non-Destructive Analyses

2 – BR2 Reactor Department

SCK•CEN, Boeretang 200, B-2400 Mol - Belgium

ABSTRACT

The swelling of the fuel plates used in research reactors can have a significant effect of the maximum fuel temperature reached during the irradiation cycle and can lead under certain conditions to cladding blistering and plate failure. The plate swelling is the result of multiple physical phenomena, including fuel burnup, interaction layer formation, and oxide layer growth, which in turn affect the fuel and cladding temperatures and the fission gas pressure. As detailed fuel plate swelling measurements became available from the E-FUTURE-1 experiment and 3-D multi-physics analyses of this experiment were performed using more accurate and experimentally validated fuel behavior models, it is possible to validate the fuel plate swelling models in the context of the E-FUTURE-1 experiment analyses. A Computational Fluid Dynamics (CFD) model based on the STAR-CD code and the SIMDIF Fuel Behavior (FB) model for the simulation of UMo dispersion are used at Argonne National Laboratory (ANL) for the analysis of the E-FUTURE-1 fuel irradiation experiment conducted in the BR2 reactor at SCK•CEN in Belgium. The fuel plate swelling results obtained from a multi-physics simulation of the E-FUTURE-1 three irradiation cycles are compared with the corresponding experimental results obtained from post-irradiation plate swelling measurements. Plate swelling model enhancements including a simplified cladding creep model are shown to improve significantly the agreement between the measured and calculated plate swelling results. The relationships between the fuel plate swelling, oxide layer growth, and the fuel meat and cladding temperatures during the E-FUTURE-1 experiment are examined.

1. Introduction

The effort to develop dispersed UMo LEU fuel elements with densities up to 7.5 - 8.5 gU/cm³ is currently focused on the qualification of LEU fuel elements at high heat-fluxes for use in the BR2, RHF, and future JHR high flux reactors [1]. The high-heat-flux irradiation test named E-FUTURE-1, consisting of 4 full-size flat plates in a dedicated irradiation basket, started in March 2010 and was completed in October 2010 in the BR2 reactor at SCK-CEN. The plates containing dispersed UMo in an Al-Si matrix were irradiated at heat fluxes up to 470 W/cm² at BOL. The non-destructive and destructive measurements of the fuel plates provided valuable information about the fuel plate behavior during irradiation which is now being used to guide the development of analytical models. The non-destructive examination of the fuel elements showed significant plate swelling and oxide film formation, and the destructive examination confirmed the oxide film formation and showed substantial changes in the fuel structure. The integrated Computational Fluid Dynamics (CFD) and Fuel Behavior (FB) model [2] developed at ANL with the goal of providing a predictive fuel performance tool was used to simulate the E-FUTURE-1 experiment. The experimentally measured changes in the fuel composition and fuel plate dimensions were compared with the corresponding calculated results in [3]. Good agreement between the calculated results and measured data was obtained for the fuel meat composition. Reasonable agreement was obtained for the fuel plate swelling, with the exception of the blister locations. A comparison of the measure oxide layer thickness with the results of simulations using an extended oxide growth model was presented in [4] showing reasonably good agreement between the calculated and measured results.. In this paper we describe recent enhancements of the fuel plate swelling model used in the multi-physics E-FUTURE-1 simulation which lead to improved prediction of the fuel plate swelling in the blister regions.

2. The E-FUTURE-1 Experiment and the Power History

The E-FUTURE-1 irradiation test was designed to allow the selection of the best combination of parameters for the LEU UMo in terms of Si content and thermal treatment. It consisted of irradiating four full size flat fuel plates contained in a specially designed basket in the BR2 reactor at high heat fluxes and then in assessing their performance parameters through non-destructive and destructive post-irradiation examinations. A schematic cross-section through the fuel basket and cross-sections through the fuel plate are shown in Figures 1 and 2, respectively. The coolant flow enters at the top of the irradiation basket with a nominal temperature of 38 C and flows downward between the fuel plates, exiting at the bottom of the basket. A thicker Al plate installed at the center of the coolant channel, parallel to the fuel plates provides additional rigidity, as shown in Figure 1.

The E-FUTURE plates are full size, high density, flat fuel plates made of dispersed UMo in Al-Si matrix (8 gU/cm³, 19.7 % ²³⁵U enrichment) with two different cladding types (AG3-NET as used in BR2 and AlFeNi as used in RHF). An important parameter for the E-FUTURE fuel plates was the Si content in Al matrix required to stabilize the interaction layer formed between the UMo and the Al matrix. Two plates - 6111 and 6301 - had 6 wt%, and the other two plates – 4111 and 4202 – had 4 wt% Si content.

The power history experienced by the E-FUTURE plates during irradiation in the BR2 reactor is an important input of the coupled CFD-FB simulations. The E-FUTURE power history was obtained from neutronic calculations of each BR2 operating cycle, based on the actual operating history of BR2 (power and control rods positions versus time during irradiation) and on the actual loading scheme of the fuel and uranium fission targets in the reactor core during each cycle [2]. The irradiation of the E-FUTURE basket in BR2 continued for three cycles during which the fuel burn-up and power changed significantly. The calculated spatial power distributions were provided to the CFD-FB simulation for the beginning, middle, and for the end of each cycle.

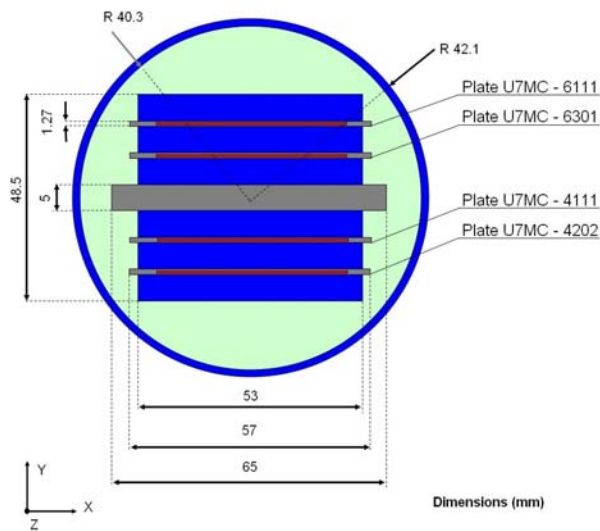


Figure 1 Cross section of the E-FUTURE basket with four U7Mo fuel plates

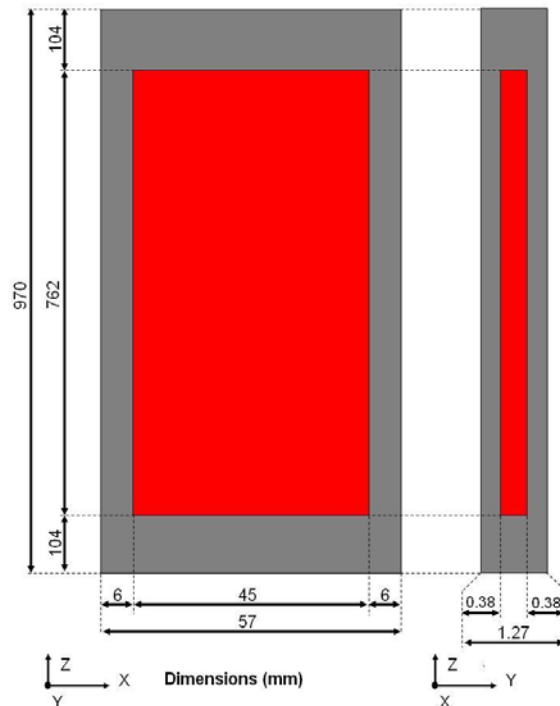


Figure 2 E-FUTURE fuel plate and fuel meat dimensions

3. The Integrated CFD-FB Model of the E-FUTURE-1 Experiment

The CFD model, based on the commercial Star-CD code, describes the irradiation basket, containing the four fuel plates and the coolant channels. The initial model geometry is the original geometry of the fuel plates before irradiation illustrated in Figure 2. The thickness of the fuel meat and cladding can change during the irradiation, as described in Section 5 below. The CFD model includes conjugate heat transfer, calculating both the thermal-hydraulic conditions of the coolant and the temperatures in the solid fuel plates and basket. The power generation in the fuel plates at a specified time during the irradiation cycle is based on the results of neutronic calculations performed for that time.

The fuel behavior (FB) model SIMDIF (Simulation of Dispersed Fuel), evaluates the changes in the geometry and thermo-mechanical properties of the fuel "meat" and cladding of the four full size fuel plates during irradiation. In order to get an accurate spatial solution, SIMDIF used the same mesh in the fuel region of the plates as the CFD model mesh. SIMDIF describes the sequence of phenomena that occur in the fuel plate during irradiation including: a) oxide layer growth, b) fuel particle swelling, c) interaction layer (IL) growth, d) fission gas generation, e) fuel plate swelling due to fission gas pressure, f) fuel meat porosity changes, and g) fuel meat conductivity changes. These models have been described in [2, 3, 4]. The extended fuel plate swelling model is discussed in Section 5 below.

To capture the interactions between the fuel mechanics and thermal-hydraulic effects during the E-FUTURE-1 experiment, each of the three irradiation cycles was divided into two discrete time intervals, resulting in six time intervals as shown in Table 1. For each time interval, a CFD calculation is performed at the mid-point of the time interval, using a power distribution obtained by averaging the beginning- and end-of-interval power distributions. This calculation determines the mid-interval fuel meat temperatures and plate-coolant interface temperatures which are then provided to the FB model. Using this information, the FB model calculates the changes in the fuel conductivity, fuel meat swelling, and cladding oxide growth during the time interval. This information is sent back to the CFD model, which uses the information received from the FB model to change the fuel plate and coolant channel geometry, and then calculates the new thermal-hydraulic conditions. More details about the coupling between the CFD and FB models can be found in [2].

Table 1 Time intervals for the E-FUTURE experiment simulation

Interval number	Irradiation cycle	Interval limits	Maximum ²³⁵ U BU [%]
1	310	day 1 (BOC) - day 7	10
2	310	day 8 - day 26 (EOC)	31
3	410	day 1 (BOC) - day 7	39
4	410	day 8 - day 28 (EOC)	55
5	510	day 1 (BOC) - day 10	64
6	510	day 11 - day 20 (EOC)	71

4. Post-test Fuel Plate Swelling Measured Results

The non-destructive PIE of the E-FUTURE plates at SCK•CEN was performed with the BONAPARTE measurement bench [5, 6]. Non-destructive analyses included plate thickness and oxide thickness measurements over the entire plate surface. Plate thickness measurements are done using two opposed, customized Sony Magnescale contact probes, whose measurement principle is based on a magnetic ruler. Ceramic thickness reference samples are used to calibrate the probes. For the measurements on the E-FUTURE fuel plates, a measurement grid of 5×1 mm was adopted, with

measurement points every 1mm in the longitudinal plate direction. A line scan was performed every 5mm in the transversal plate direction. Detailed scans, using a 1x1 mm² grid were recorded in the blistered areas of each fuel plate.

All four E-FUTURE plates show important swelling in the highest burnup region. The measured results are visualized in the 2D contour plots shown in Fig. 3 for all plates. The 6XXX plates which have 6 wt% Si content show a smaller maximum swelling in the pillowed areas than the 4XXX plates which have 4 wt% Si content.

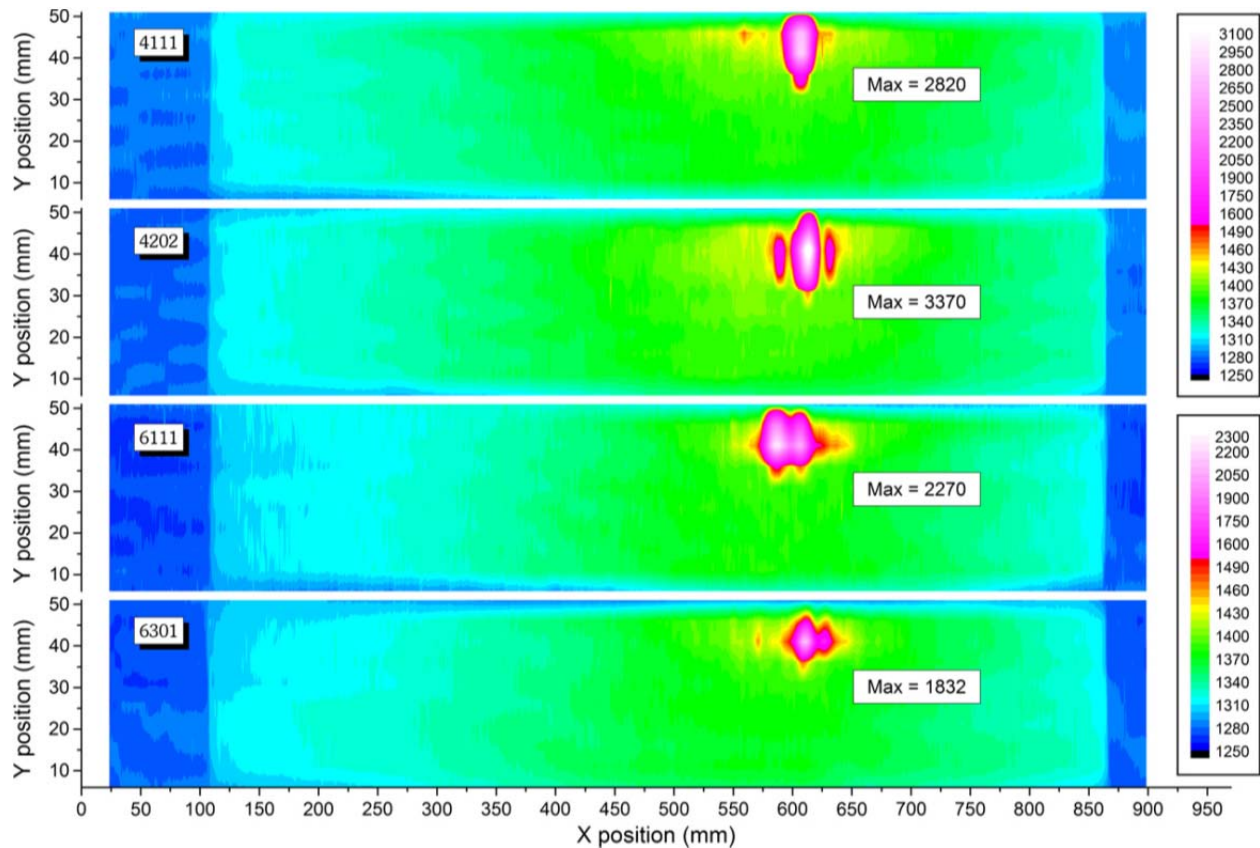


Fig. 3 Plate thickness contour plots as measured (uncorrected). Colour scales are adapted to show the 'normal' swelling (1250–1500 μm) and the pillowing (>1500 μm). Color scale in μm. [Ref 5]

5. The Extended SIMDIF Fuel Plate Swelling Model

In SIMDIF, the fuel plate swelling is assumed to be determined by both the fuel particle swelling and the fission-gas-driven pressurization of the interaction layer (IL). The forces due to these phenomena act simultaneously on the cladding at each mesh location to determine the local plate swelling as illustrated in Figure 4. The models that determine the two plate swelling components are described in more detail below.

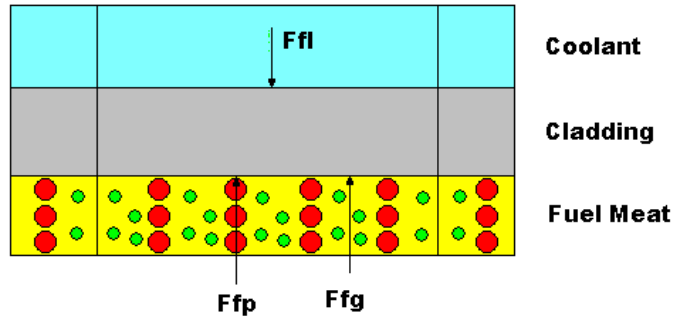


Figure 4 Forces Acting on the Cladding in the SIMDIF Model: a) Inner Fuel Particle Force F_{fp} , b) Inner Fission Gas Force F_{fg} , and c) Outer Fluid Force F_{fl} (red=fuel particles, green=fission gas filled pores)

5.1 Fuel Plate Swelling due to Fuel Particle Swelling

The fuel particle swelling component of the plate swelling is determined primarily by the local fuel burnup. The total fuel particle swelling due to irradiation is calculated using a correlation developed at Argonne National Laboratory [7] which depends only on the local fission density. This correlation has been built mainly on the numerous irradiation tests of UMo monolithic fuel in which there is no interaction between the fuel and aluminum. The fuel particle swelling is considered to be the sum of two contributions: swelling due to solid and gaseous fission products. Both phenomena only depend on the local fission density. The volume of gaseous fission products inside a fuel particle is considered as porosity and is taken into account in the modeling of the IL formation, as discussed in Section 5.2 below. The fuel particle swelling is calculated as:

$$\frac{\Delta V}{V_0} = 5.0 \times f_d \quad \text{for } f_d \leq 3.0 \quad (1)$$

$$\frac{\Delta V}{V_0} = 15.0 + 6.3 \times (f_d - 3.0) + 0.33 \times (f_d - 3.0)^2 \quad \text{for } f_d > 3.0 \quad (2)$$

Where the fuel swelling $\frac{\Delta V}{V_0}$ is in percent and the fission density f_d is in 10^{27} fissions/m³.

SIMDIF assumes that the size of the fuel particles is determined solely by the fuel particle swelling and the fuel particle swelling leads to the fuel plate swelling. This assumption leads to good plate swelling prediction in regions away from the blister region. However, the fuel particle swelling alone cannot explain the large swelling observed in the blister region [3].

5.2 Fuel Plate Swelling due to IL Fission Gas Pressure

The overall SIMDIF plate swelling model allows for an additional plate deformation mechanism driven by the fission gas pressure in the interaction layer. The swelling component due to fission gas pressure is strongly dependent on the local IL, matrix, and cladding conditions. The IL region separates the fuel particles and the matrix and contains the interaction compounds and the fission-gas-filled pores or bubbles. The fission gas pressure in the IL region is determined by the amount of fission gas present, local temperature, and available pore volume.

The fission gas present in the IL region is assumed to be contained in large bubbles or pores, so that the effect of surface tension on the gas pressure can be neglected. It is noted that, with this assumption, the actual size or location of the individual bubbles in the IL region - e.g. bubbles can accumulate at the IL region boundaries with the fuel or matrix - is not necessary for the fission gas pressure calculation. The fission gas pressure in the IL region is determined by the amount of fission gas present, local temperature, and available pore volume. using the perfect gas equation:

$$P_{fg} = \frac{M_{fg} \times R \times T_{fu}}{m_{fg} \times V_{gas,IL}} \quad (3)$$

Where M_{fg} is the mass of fission gas in the IL, R is the perfect gas constant, T_{fu} is the local fuel temperature, m_{fg} is the fission gas molar mass, and $V_{gas,IL}$ is the volume of the large gas bubbles in the IL region.

The local fuel temperature T_{fu} is obtained from the CFD model, while the mass of fission gas in the IL region M_{fg} and the volume of the porosity in the IL region $V_{gas,IL}$ are obtained from the IL growth models described below.

5.2.1 Interaction Layer Growth Models

The growth of the matrix–fuel Interaction Layer (IL) depends of several factors including irradiation time, local fission rate and local fuel meat temperature. Empirical correlations have been developed at ANL in order to model the IL growth [8] and are updated when new experimental data becomes available. The correlation used to model the growth of the interaction layer includes also the effect of silicon content in the aluminum matrix as shown in Eq. 4.

$$Y_{IL}^2 = 2.6 \times 10^{-8} \times f^{0.5} \times \exp\left(\frac{-3850}{T}\right) \times t \times f_{Si} \quad (4)$$

Where Y_{IL} is the IL thickness in μm , f is the fission rate in fissions/(cm³-s), T is the local fuel temperature in K, t is the irradiation time in seconds, and f_{Si} is a correction factor that accounts for the effect of Silicon content in the matrix

The increase in the interaction layer calculated with Eq. (4) is divided into two regions,

as illustrated in Figure 5: a) a fuel region FR at the IL-fuel particle boundary, which leads to the decrease of the fuel particle volume, and b) a matrix region MR at the IL-matrix boundary, which leads to the decrease of the matrix.

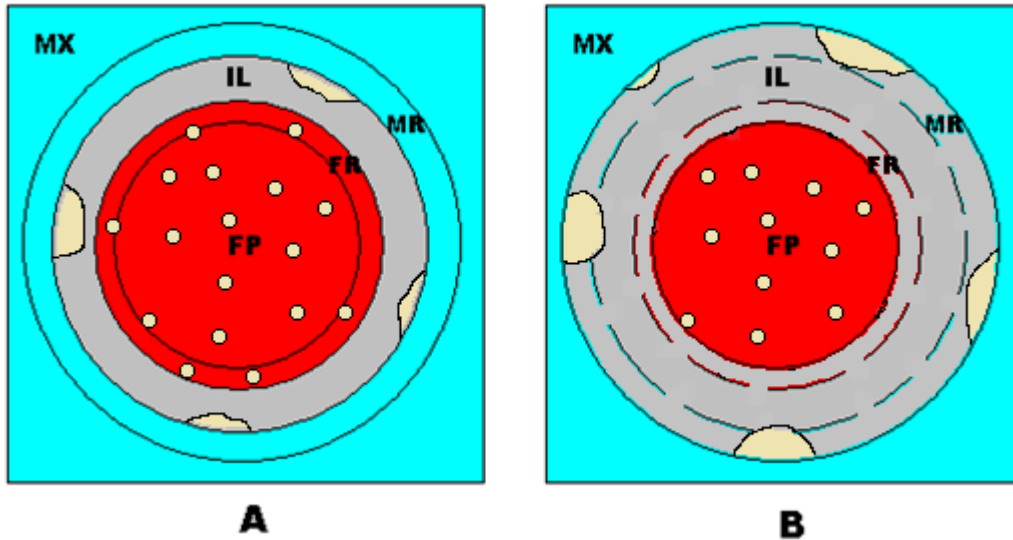


Figure 5 Interaction Layer Growth: a) IL region at the Beginning of Time Step, and b) IL region at the End of Time Step. (grey - interaction layer IL, red - fuel particle FP, blue - matrix MX, yellow – Fission Gas)

The fuel and fission gas present if the FR region of the fuel particles become part of the interaction layer. The fission gas contained in the FR region pores is added to the mass of fission gas in the IL M_{fg} and the volume of the fuel particle pores contained in the FR region is added to the volume of the gas bubbles in the IL $V_{gas,IL}$. The Al-Si and the pores present if the MR region of the matrix also become part of the interaction layer. The volume of the matrix pores contained in the MR region is added to the volume of the gas bubbles in the IL $V_{gas,IL}$. The mass of fission gas in the IL M_{fg} also increases due to the addition of fission gas produced by fissions that occur in the IL.

5.2.2 Forces acting on the cladding and Plate Swelling

The forces F_{fg} and F_{fl} acting on the on the inner and outer face of the cladding respectively, at a given location are calculated as follows:

$$F_{fg} = P_{fg} \times A \quad (5)$$

$$F_{fl} = P_{fl} \times A \quad (6)$$

Where: P_{fg} is the fission gas pressure in the IL region, P_{fl} is the coolant pressure on the outer face of the cladding, and A is surface of the un-deformed cladding in the given cell.

The SIMDIF initial model evaluating the local plate deformation due to the fission gas

pressurization of the IL was a first step toward building a mechanistic plate swelling model. It assumes that the aluminum matrix provides no resistance to swelling and that all the resistance to swelling is due to the cladding. A value representative of the Local Stress (LS) acting on the cladding is calculated using the net force exerted on the cladding by the internal force due to the fission gas pressure F_{fg} and the external force due to the coolant fluid pressure F_{fl} as shown in Eq. 7:

$$LS = (F_{fg} - F_{fl}) / A_L \quad (7)$$

Where: A_L is the area of cladding cell surfaces that separate a given mesh cell from the neighboring cells, calculated as $P \times T$, where P is the perimeter of the cladding cell and T is the cladding thickness for that cladding location.

Since this component of the total deformation is assumed to occur mainly in the plastic regime, the LS is compared to an effective yield stress (EYS) calculated as follows:

$$EYS = Ceys * YS(T) \quad (8)$$

Where: $YS(T)$ is the temperature-dependent yield stress of the cladding and $Ceys$ is a user selected parameter that accounts for effects not explicitly considered in this simplified approach used to calculate the cladding deformation. The value of $Ceys$ ($Ceys = 0.01$) was obtained through calibration with the E-FUTURE-1 plate swelling measurements obtained for the plate 6301. Only one plate (6301) was used for model calibration, and the results for the other three plates (6111, 4111, and 4202) were used to evaluate the predictive capability of the model.

When the calculated local stress LS exceeds the value of EYS, the volume of the fission gas bubbles – and the plate thickness - is increased, thus reducing the pressure F_{fg} and the local stress until:

$$LS = EYS \quad (9)$$

As mentioned above, this component of the deformation is assumed to occur mainly in the plastic regime. The swelling due to the IL region fission gas pressure is zero or very limited at lower burnup values, when the plate swelling is determined solely by the swelling of the fuel particles as described in Section 5.1 above. As the fission gas pressure increases during irradiation and the cladding resistance decreases due to the oxide layer growth, this plate swelling component becomes increasingly important and can lead to large local plate deformations.

The SIMDIF plate deformation model was then extended in order to describe the creep deformation that could occur as a result of long exposure to a high stress that remains below the yield strength of the cladding. It is expected that this type deformation could be more prevalent at temperatures that are a significant fraction of the melting temperature. For cladding temperatures below $T_{creep}=395$ K, the model assumes that the creep effects are limited and the component of deformation resulting from the

pressurization of the IL is calculated as in the original model. At temperatures above T_{creep} the yield stress $YS(T)$ in Eq. 8 is replaced by a creep stress $CS(T)$, which causes the creep strength to decrease rapidly to values that are approximately an order of magnitude lower than the yield strength. The underlying assumption is that the creep accelerates and becomes fast enough to allow the forces acting on the cladding to reach an equilibrium condition during the irradiation time step considered, i.e. to cause cladding deformation until the stress due to interaction-layer fission gas pressure is equal to the creep strength. The 395K threshold value is based on Ref. [9] but it is acknowledged that it does not necessarily correspond to the E-FUTURE-1 cladding properties. This value will be modified when more accurate cladding data becomes available.

6. Results of Fuel Plate Swelling Simulations

The SIMDIF fuel plate swelling model described above has been used to simulate the fuel plate response during the E-FUTURE-1 irradiation experiment. Because the fuel plate swelling component due to fission gas pressurization is highly dependent on the models describing the changes that occur in the fuel meat and on the oxide layer growth which affects the cladding thickness and temperature, we evaluated in previous work the accuracy of the SIMDIF models that describe these phenomena. It was shown in [3] that the calculated changes that occurred in the fuel meat during the E-FUTURE-1 simulation are in good agreement with the corresponding post-test destructive analysis results. The extended oxide growth model was validated in [4] and showed to provide results that are in good agreement with the corresponding PIE destructive and non-destructive measurements. Fuel plate swelling simulations performed with the initial fission-gas pressure swelling model that did not include the creep swelling model predicted swelling that was in good agreement with the corresponding post-test measured values over most of the plate surface, but did not predict the large local swelling or “blisters” observed in the experiment, as illustrated in Figure 6.

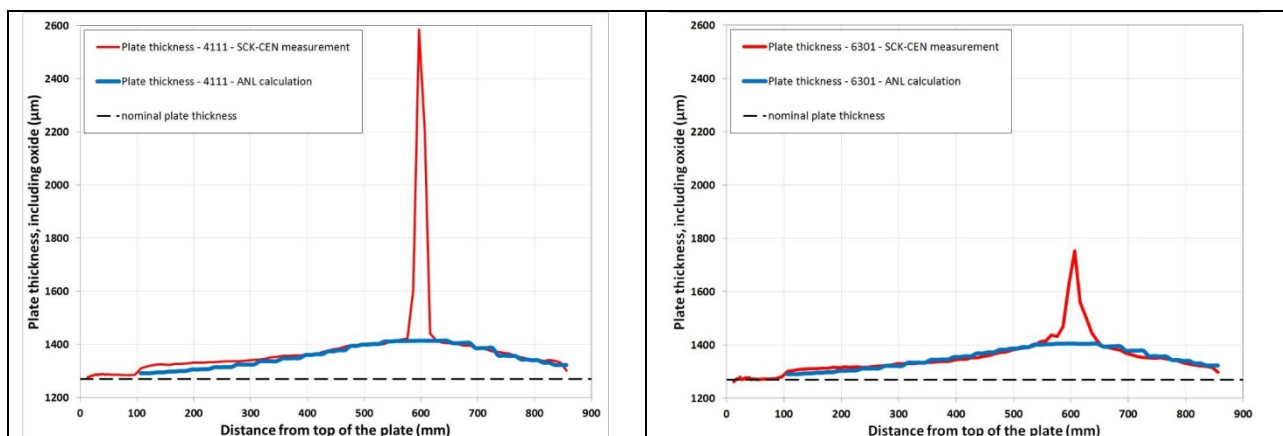


Figure 6 Fuel Plate Thickness vs. Distance from Top of the Plate, at 10 mm from the High Power Edge, for Plates 4111 (left) and 6301 (right). Red – measurement, Blue – Calculation before the addition of the creep swelling model [Ref 3]

Plate swelling results calculated with the expanded plate swelling model, which includes the creep swelling model described in Section 5 above are shown in Figure 7 (in blue) and compared with the corresponding experimental data (in red). The swelling results obtained without using the creep swelling model are also included (in green). The figure shows the plate thickness increase at 10 mm from the high-power edge, along the plate length.

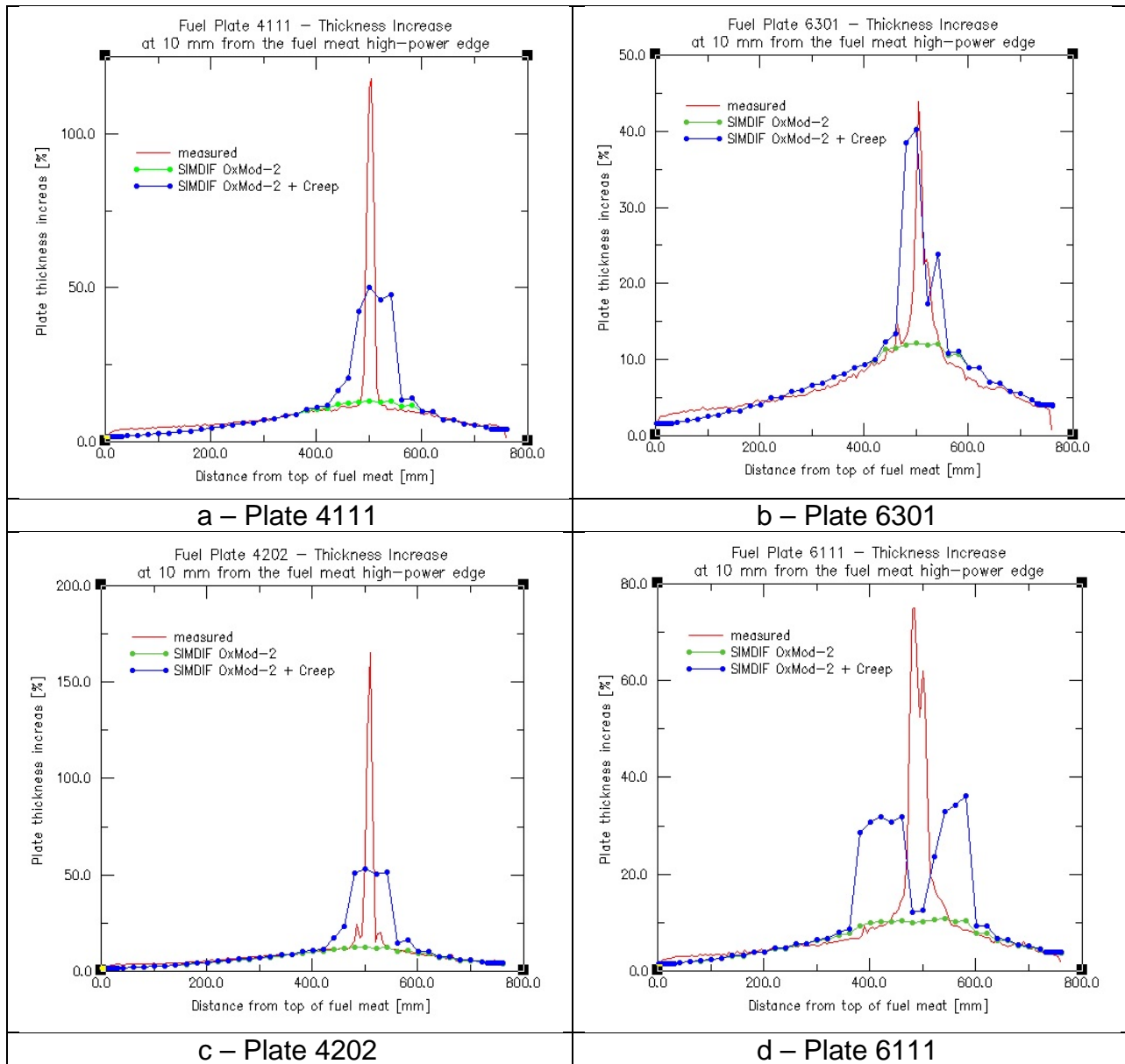


Figure 7 Comparison of E-FUTURE-1 Plate Swelling Calculated with the SIMDIF extended plate swelling model with the measured data

The best agreement between calculated and measured swelling is obtained for plate 6301 (Figure 7b). The calculated blister location, height, and width are all in good

agreement with the observed data. This is partially due to the fact that a limited calibration of the creep swelling model was performed using the plate 6301 swelling data. No further model calibration was performed for the other plates. The location of the blister is predicted reasonably well for plates 4111 and 4202. But for both plates the calculated blister height is lower than the measured value and the calculated blister width is higher than the measured value. Finally, the two-peak blister predicted for plate 6111 shows the less agreement with the data than the other plates, although a two-peak structure of the measured blister can be observed for plate 6111 in Figures 7 and 3. It is noted that the plate 6111 was the only E-FUTURE-1 plate that was rotated between the 2nd and 3rd irradiation cycles. Although this rotation is included in the CFD-FB simulation, the reduced agreement between the calculated and measured swelling for this plate is likely due to the more complex irradiation history.

The extended swelling model predicts the blister formation during the irradiation for all the four plates irradiated in the E-FUTURE-1 experiment, in agreement with the observed experimental results. The blister location prediction is generally good, and the predicted blister height varies from ~30% of the observed height for the highest blister (plate 4202) to ~100% of the observed height for the lowest blister (plate 6301). In relation to the plate thickness the predicted blisters vary between 40% - 50% percent of the original plate thickness and are easily recognizable as excessive local swelling.

7. Conclusions

The SIMDIF plate deformation model was extended to include a simplified creep model, in order to describe the possible creep deformation that could occur as a result of long exposure to a high stress that remains below the yield strength of the cladding. It is expected that this type deformation could be more prevalent at temperatures that are a significant fraction of the cladding melting temperature. Analyses of the E-FUTURE-1 experiment performed with the extended SIMDIF plate swelling model predict plate swelling that is in reasonably good agreement with the observed data. Large blister-like local plate deformations are predicted for all four E-FUTURE-1 plates in agreement with the experimental observations. Future work will focus on the extension of the SIMDIF models to describe the response of the fuel plates with coated fuel particles used in the SELENIUM irradiation experiment. The analysis of additional LEU fuel irradiation experiments is planned in order to confirm the predictive capability of the models.

8. References

- [1] F. Frery et al., "LEONIDAS U(Mo) Dispersion Fuel Qualification Program: Progress and Prospects," Proceedings of the 32nd International Meeting on Reduced Enrichment for Research and Test Reactors, Lisbon, Portugal, October 10-14, 2010.
- [2] A.M. Tentner, A. Bergeron, Y.S. Kim, G.L. Hofman, J.G. Stevens, "An Integrated Computational Fluid Dynamics and Fuel Mechanics Model for the Analysis of the E-FUTURE Fuel Irradiation Experiment", Proceedings of the 33rd International Meeting on Reduced Enrichment for Research and Test Reactors, Santiago, Chile, October 23-27, 2011.
- [3] A.M. Tentner, A. Bergeron, Y.S. Kim, G.L. Hofman, J.G. Stevens, S. Van den Berghe, V. Kuzminov, "Multi-Physics Simulation of the E-FUTURE-1 Fuel Irradiation Experiment", Proceedings of the 34th International Meeting on Reduced Enrichment for Research and Test Reactors, Warsaw, Poland, October 14-17, 2012.
- [4] A.M. Tentner, A. Bergeron, Y.S. Kim, J.G. Stevens, S. Van den Berghe, V. Kuzminov, "Modeling of the Cladding-Oxide Growth and its Effects on the Thermo-Mechanical Performance of the Fuel Plates in the E-FUTURE-1 Experiment", Proceedings of the European Research Reactor Conference RRFM 2014, Ljubljana, Slovenia, April 2014.
- [5] S. Van den Berghe, Y. Parthoens, F. Charollais, Y. S. Kim, A. Leenaers, E. Koonen, V. Kuzminov, P. Lemoine, C. Jarousse, H. Guyon, D. Wachs, D. Keiser Jr, A. Robinson, J. Stevens and G. Hofman, Journal Of Nuclear Materials 430 (1-3), 2012.
- [6] S. Van den Berghe, A. Leenaers and Y. Parthoens in: Proceedings of the International Meeting On Reduced Enrichment For Research And Test Reactors (RERTR), Santiago, Chile, October 2011.
- [7] Y.S. Kim, G.L. Hofman, "Fission product induced swelling of U-Mo alloy fuel", Journal of Nuclear Materials 419, 2011.
- [8] Y.S.Kim et al, "Modeling of Interaction Layer Growth between UMO particles and an Al Matrix", Nuclear Engineering and Technology 45(7), December 2013.
- [9] D.M. Royster, "Tensile Properties and Creep Strength of three Aluminum Alloys Exposed up to 25,000 hours at 200 F to 400 F", NASA technical Note NASA TN D-5010, Washington, D.C., January 1969.